SINERGI Vol. 25, No. 3, October 2021: 371-380
http://publikasi.mercubuana.ac.id/index.php/sinergi
http://doi.org/10.22441/sinergi.2021.3.014

TRIBOLOGICAL PROPERTIES OF AL_2O_3-ZrO_2 COMPOSITE COATING BY LUBRICATION

Riyadh A. Al-Samarai[1], Haftirman[2]*
[1]Electromechanical Engineering Department, Engineering College, University of Samarra, Iraq
[2]Department of Mechanical Engineering, Faculty of Engineering, Universitas Mercu Buana, Indonesia

Abstract
Tribological investigations had been carried out on the plasma coating (Al_2O_3+ ZrO_2) below dry and moist abrasion stipulations according to ASTM G134. Commercial motor oil 20W40 was used as a lubricant. At a rotational speed of 200 rpm, all experiments were carried out with ordinary loads of 10, 15 and 20 Nm. Electron microscopy for scanning and AFM was used to study the layer sprayed with paint. The SEM and AFM evaluation outcomes confirmed that abrasive wear is normally decided by abrasive wear in dry abrasive conditions. The lubrication and moisture check confirmed a major reduction in wear from 10 to 15 N below regular loading, and a corrosion fee larger than 15 N was once discovered below regular loading. No impact of lubrication on wear used to discovered at high loading. No impact of lubrication on wear used to be discovered at high loads. It was also cited that the plasma coating manner improves wear resistance. The experimental statistics acquired in this study are tremendous engineering functions such as reducing equipment and internal combustion engines.

Keywords:
Abrasive wear;
Lubricant;
Plasma coating;
Tribological;

Article History:
Received: February 10, 2021
Revised: April 15, 2021
Accepted: May 17, 2021
Published: August 10, 2021

Corresponding Author:
Haftirman
Department of Mechanical Engineering, Faculty of Engineering, Universitas Mercu Buana, Indonesia
Email: haftirman.haftirman@mercubuana.ac.id

INTRODUCTION

Over the previous three decades, many scientific and technical barriers to historically used ceramics have been removed. Various substances such as Y_2O_3, ZrO_2, and Al_2O_3 are combined with distinctive stabilizers such as BeO, SiC, AlN, Si3N4, WC, etc., or MnO, CaO used in engineering networks [1, 2, 3, 4, 5]. Despite the nature of the ceramic material, it has been efficaciously used in the oil and fuel enterprise as nicely as for airspace components, variety of reducing tools, solid fuel cells, combustion engines, etc. Due to its uncommon negativity against oxidation, excessive put-on resistance and excessive thermal stability Compared to monolithic minerals. The pure porcelain cloth does not exhibit any promising effects due to its fragile homes and limited duration [1, 2, 3, 4, 5]. However, preceding studies have proven very few outcomes while mixing easy ceramics with metallic powder can be viewed as positive. This formula is referred to as cermet [5]. To achieve a high-quality benefit and due to the fact of the mechanical thermal advantages, researchers must locate a high-quality formulation that can be utilized at high temperatures (>a thousand °C).

The ceramic cloth used to be chosen amongst scientists and engineers for the first time due to the fact of its extraordinary mechanical and thermal properties. These properties encompass chemical inactivity, excessive rigidity, corrosion resistance, and strangely sturdy covalent bonding, ensuring excessive structural integrity when used in one-of-a-kind environments (high temperature, corrosion, and friction) between components. On the other hand, the limited thermal property hyperlinks the use of homogeneous materials compared to ceramics. Furthermore, it is found that the atomic bonding in ceramics is controlled by ionic bonds acknowledged as covalent (the presence of the two sorts contributes to mixing ceramics with mineral powder). However, when it comes to minerals,

solely the bond determines the power and efficiency of the substance. This work has resulted in a tremendous increase in ceramics use compared to standard materials [6].

After reviewing the accelerated literature, it was located that the corrosion of the samples frequently depends on the microstructure of the coating and the porosity, hardness, thickness, and running conditions such as load and slip speed friction [7]. From previous studies, the method of ZrO_2 coating 8 wt% of Y_2O_3, ZrO_2 coating 20wt% of Y_2O_3, and Al_2O_3 ZrO_2 has a longer life than cast iron [8][9]. In general, it was determined that a cloth's wear resistance is always carefully associated with the defects of the coating and the hardness of the abrasive materials [9].

A necessary problem is the grain size, which has a principal effect on its resistance to corrosion [10, 11, 12]. Besides, it was discovered that the composite materials had a high impact on the wear manner [13]. Aluminum crystalline polyurethane is usually corrosive and varies radically in accordance with the common grain size. As a result, the average wears price increases hastily with grain measurement [14][15]. Previous studies have proven that the granular material is less corrosive than coarse porcelain [15]. Wang [16] studied the corrosion residences of a nano-structure titanium alumina coating on a mild metal substrate (16 to 600 nm). His learn showed that the worn surfaces of typical painting tactics produce grooves as nicely as plastic deformations and exceptional refractive processes.

However, the control procedure for extracting nanostructured coatings used to be discovered to be related to the grain separation procedure [17]. Lee Van performed erosion studies on types of ZTA covered iron matrix compounds and observed a 30-volt compound. Percent of ZTA particles confirmed the great resistance during put on test [18]. Friction and put on analyzes have been carried out on the Fe-Ni alloy matrix (Fe70Ni30). Percent ZrO_2 of particles had been detected and added 10 wt. ZrO_2% elevated wear resistance and decreased plastic drift during put on [19]. Recently, a range of laboratory lookup studies on the formation of calcium-stable zircon and alumina ceramics ($Al2O_3$ + ZrO_2) have been studied and studied. Good outcomes were got in phrases of excessive anti-corrosion thickness from 200 to 300 nm. The massive improvement in adhesive power used to be (49.33 MPa). For Al_2O_3, a 3% reduction in satisfactory porosity was once determined compared to about 10%. The lifestyles of the coating used to be elevated (312 cycles of heating and cooling inside 1/2 an hour of time) and the thickness used to be elevated to 300 nm after undergoing periodic thermal assessments [20][21].

The process of utility and understanding of this above ceramic shape is still below investigation and requires, in addition, lookup and development. Due to the response of the composite ceramic material, a few researchers have sought choice configurations. Intensive lookup on Al_2O_3 + ZrO_2 blended methods is underway. In this regard, a find out was once carried out to find out about the behavior of this paint in dry and moist conditions and beneath unique loading conditions. Different ranges of put on have been compared. Also, the first-rate (wear resistance) has been detailed for a specific load and can be applied to inside combustion engines or slicing machines.

Due to the response of the composite ceramic material, a few researchers have sought choice configurations. Intensive lookup on Al_2O_3 + ZrO_2 blended methods is underway. In this regard, a find out about was once carried out to find out about the behavior of this paint in dry and moist conditions and beneath unique loading conditions. Different ranges of put on have been compared. Also, the first-rate (wear resistance) has been detailed for a specific load and can be applied to inside combustion engines or slicing machines.

METHOD

Specimen preparation

The sample was covered with a plasma coating. Eighteen samples (pigments produced on forged iron) have been organized and painted to study put on the rate. The approximate dimensions of each pattern have been made appropriate for the experimental test. The sample profile is proven in Figure 1.

Material facts for plating applied to forged iron and working stipulations are given in Table 1. The working conditions considered during the test are given in Table 2.

The mean value of the coating thickness was set to 200 ± 32 μm. The coating thicknesses scheme is presented and discussed in Methodology.

Coating Characterization

A detailed examination was conducted of the structure of microscopic; particle size for all surfaces worn and sprayed using optical electron microscopy. The properties of the model are given in Table 3.

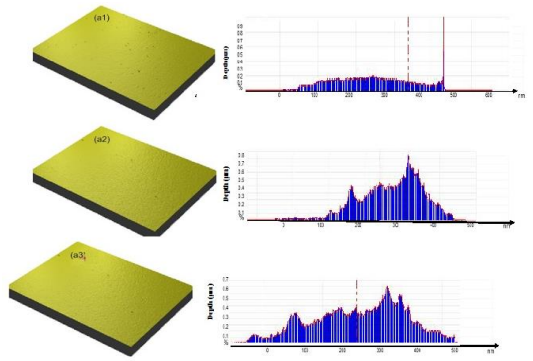

Figure 1. AFM for plasma sprayed coated specimen (15×15 mm^2) and micro-topography of the surfaces and roughness profiles of the wear tracks after test (a1) Ra= 1.18 ± 0.05 µm (a2) Ra= 7± 0.05 µm (a3) Ra= 8.20 ± 0.05 µm, at speed 3 mm/s

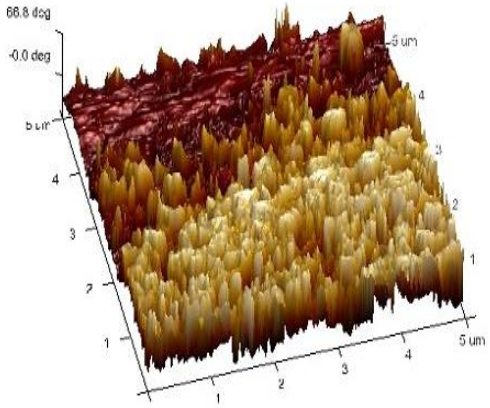

Figure 2. AFM of cross section of topcoat thickness

SEM analysis

Scanning Electron Microscopy (SEM, SU 3500N, Hitachi) and were used to denote displacement morphology and coverage area. The average roughness along the center line Ra of the coatings used on the wafer is achieved at a distance of 1 µm. The defined structure of carbon atoms in the coatings is used for atomic pressure microscopy (AFM) (USA, ESCALAB 250Xi, Thermo Scienti - Fc XPS), which is used to analyze the states of coatings are given in Figure 2.

Wear Analysis

ASTM G132 [22] has been adopted in all abrasive put on tests. In abrasive wear, a 60 micro grinding disc is set up on the put-on machine. During the Tribology test, the loss of coatings (shortening of the pinnacle layer of the coating) was once bought from the data-readout system immediately linked to the laptop, as depicted in Figure 3(a).

Data was once used by using the application as properly as the formula (see below) to decide the sum of quantity loss over the designated sample.

Table 1. Composition and Parameters

Materials	Primary gas (Argon) Pressure (Bar)	Secondary gas (Hydrogen) Pressure (Bar)	Carrier gas Argon Flow (lpm)	Current (Amps)	Voltage (Volts)	Spray distance
Al_2O_3	3,7	3,45	35	00	65	65-76

Table 2. Operating parameters

Operating parameter	
Normal load	10,15 and 20 N
Disk speed	200 rpm
Track diameter	60 mm
Abrasive grain size	60 µm
Type of lubricant (commercial)	20W40 Engine Oil

Table 3 Scanning microscope specification

SEM Specification	
Make	Hitachi
Model	SU 3500N
Detector	SE and BSE
Resolution	7nm SE image at 3 kv, 10 nm BSE image at 5 kv
Voltage	Variable (up to 30kv)
Magnification	300000 X

All exams were performed at three exceptional regular loads, 10, 15, and 20 N. Loads were selected for (mainly experimental fixing restrictions) and for checking paint at loads. Under dry and moist wear conditions, three exams had been performed under each load and the put-on charge was once determined. A syringe was once used to alter the lubrication failure (motor oil) on the rotating disc shown in Figure 3(b).

The formula used to calculate specific wear rate:

$$\text{Cross-sectional area} = (\text{Sides2}) \text{ in } (\text{mm2}) \quad (1)$$

$$\text{Volume loss} = (\text{Cross-sectional area} \times \text{Average height loss}) \text{ in } (\text{mm3}) \quad (2)$$

Average height loss measurement was taken from the data generated by the software

$$\text{Sliding Distance} = [\text{Sliding Velocity } (\text{m/s}) \times \text{Time(s)}] \text{ in } (\text{m}) \quad (3)$$

$$\text{Sliding Velocity} = [(2\times\text{Pi}\times\text{N}\times\text{r})/ (60\times1000)] \text{ In } (\text{m/s}), \text{ where N= Rotational Speed of a disk in (rpm), r = Track radius in (mm)} \quad (4)$$

$$\text{Wear rate} = (\text{Volume loss}/ \text{Sliding Distance}) \text{ in } (\text{mm3/m}) \quad (5)$$

$$\text{Specific wear rate (SWR.)} = (\text{Wear rate/Normal Load}) \text{ in } (\text{mm3/mN}) \quad (6)$$

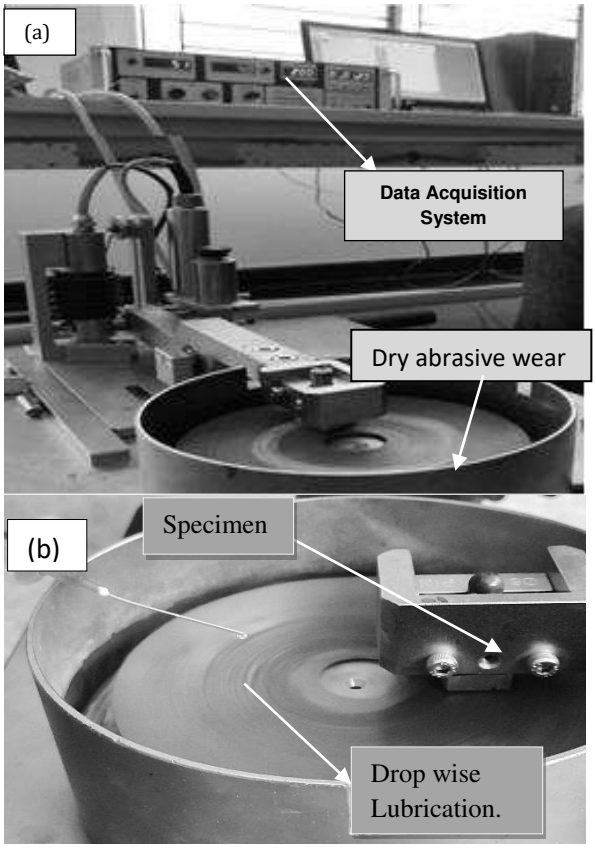

Figure 3. (a) Schematic of the tribological setup (a) Dry, condition (b) Wet condition

RESULT AND DISCUSSION

Coating Characterization

A contrast of analyzes of SEM and after coating showed how to spray hardened surfaces, suspended particles, as properly as topical particles related to materials, and the spraying coating, as shown in Figure 4(a). The microfarad of the cap was measured and discovered to be 668.9 HV. Subsequent wear analysis confirmed a surface with partial open spaces as properly, see Figure 4(b). Partially open holes and cavities with lubricants are useful in the evaluation of cutting-edge wear. It was observed that the lubricant and medium layer of tribofilm were obvious and had a clear effect on the corrosion mechanism that befell at some point of the test. In the moist state, a cover was once found floating on a tribofilm and mounted between surfaces. It was located that there used to be a decrease pressure effect on the wear route at some point of low hundreds (10-15 N).

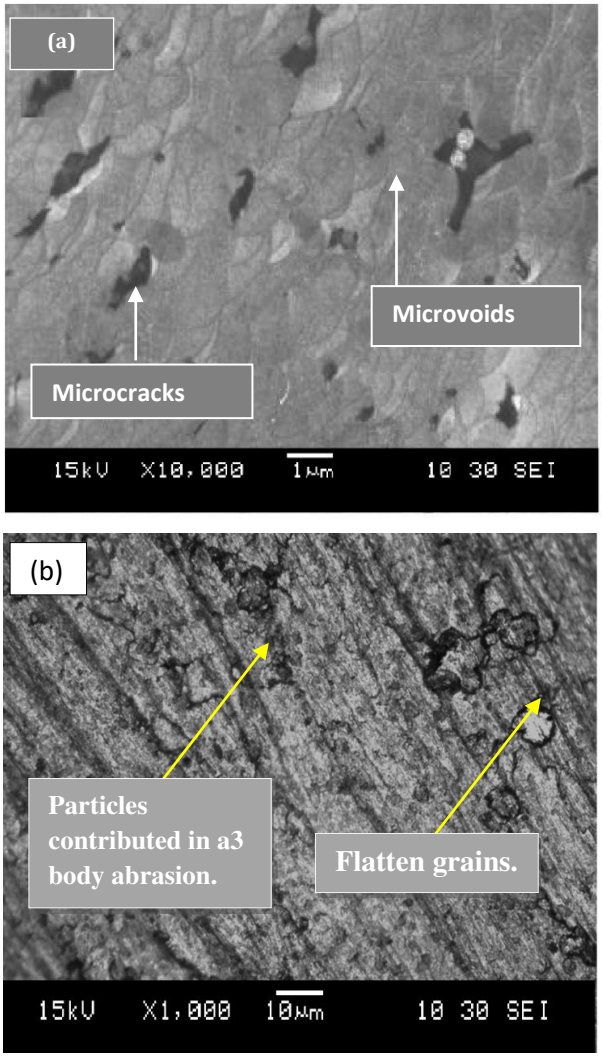

Figure 4. Schematic of topcoat status (a) As-sprayed (b) Post wear

The coating cloth's integrity is additionally validated by growing the dimensions and width of abrasion from 172 to 181 µm beneath the dry wear-out mechanism, with abrasion prerequisites below moisture, between 10-15N ordinary load with a size measured in varies 66.9 -81 mldi as shown in Figure 5. Figure 6 are proven with the aid of SEM micrograms in dry and moist conditions. In coatings, the usual particle measurement diminished from 1.81 µm to 8.20 ‹µm, on the other hand, all through the dry erosion phase (~1.69 - ~2.36 µm), the particle size diminished significantly, see Figure 4(a) and Figure 4(b), respectively. A comparable range of wet particle size (~ 1.43-2.70 µm) used to be located in wet scraping conditions. See Figure 4(c). Direct effect on the ratio of the charge of corrosion was discovered due to the decline in the exact dimension of the particles, additionally, it discovered that the erosion of aluminum acknowledged bated

crystals, as well as the fee, varies appreciably depending on the common particle measurement and accuracy. Increased wear fee rapidly with growing grain size [23].

Through preceding research showed that the porcelain with a granular measurement with a low corrosion fee compared with the corrosion of coarse granular ceramics [24][25]. It resulted in reducing the dimension of a grain of Al2O3 from 20 to 4 micrometers to extend five-fold when transferring from the average corrosion phase, which is the stage of very speedy corrosion characterized by way of erosion of plastic deformation [26]. Through this work additionally, there is assistance for the above points. The smaller the grain size, the extra correct the ensuing defects, and therefore requires a high degree of external pressure, which leads to the cracking and pulling of the grain. Small grains are greater shock resistant [27][28].

From the SEM 4 (ac) and 5 (b), it was discovered that excellent and porous gaps could contribute to the formation of tribofilm and significantly decrease put on between the mating components between the contact surfaces.

Wear Analysis

Comparative evaluation of the moist and dry case, underneath regular low load, from 10 to 15 N (case of wet), mild scarring, and the effect of erosion is important. It was measured by means of the common corrosion fee at this being pregnant and chooses between 0.026 - 0.051 × 10^{-6} mm^3 / m. However, the observed fee is slightly higher in the dry corrosion test, any of 0.047 to 0.107 × 10^{-6} mm^3 / m. It was also discovered that the common corrosion fee at excessive load (20N) dry and moist conditions are in Table 4 and Table 5 will increase significantly at least under 10N, located lubrication layer in contact with the surface. Still, no longer in loads when loading 20 N, close effects can be considered on the SEM micrograph as shown in Figure 5.

Where the measured values have been received for SEM micrographs, in wet and abrasive, take a look at conditions, it is determined that there are essential effects between 10-15 Nm loading.

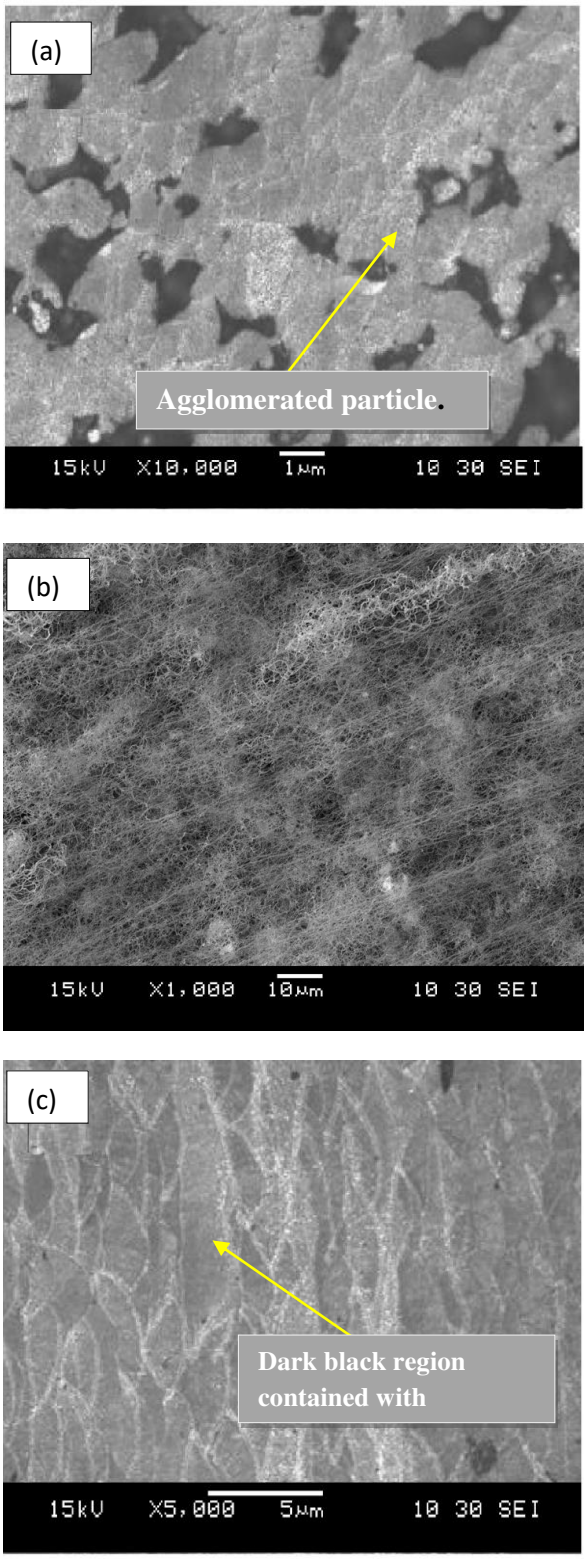

Figure 5. Topcoat particle size (a) As-sprayed, (b) Dry-Post wear and (c) Wet- post wear

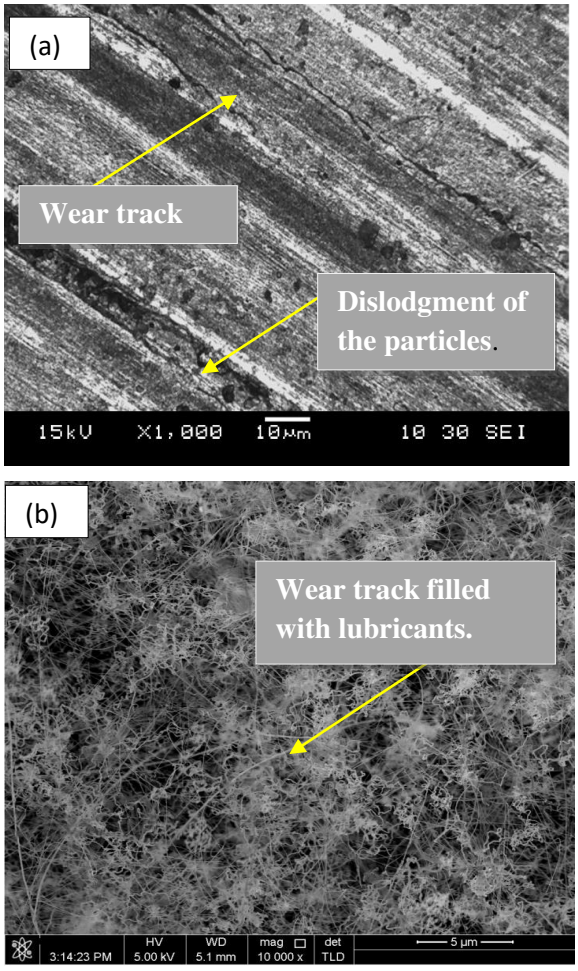

Figure 6. SEM of wear track in:
(a) dry condition (b) Wet condition

It was once located that the deformed areas (high pressure) had been underneath the take a look at of lubricants, thus forming a membrane at some point of the response forces, which reduces the load as well as the wear by way of 10-15 N. A similar scenario used to be discovered on the SN micrograph at ordinary load 20 N, see Figure 7 (c). Show in Figure 8. In Table 6, the results contrast is presented. Under the conditions of the lubrication and moist look at conditions, at 20N load, a decrease in the impact of put on and was found due to the impact of the tripoflam layer.

The reason and resultant particles to come out and soften the pattern (three corrosives to the body). The wear except lubrication used to be additionally reviewed and in contrast as proven in Figure 8. The put-on rate for everyday hundreds from 10 to 15N was once determined. On the other hand, in dry abrasive mode, the wear charge steadily increased. In each case, the wear charge used to be continuously declining.

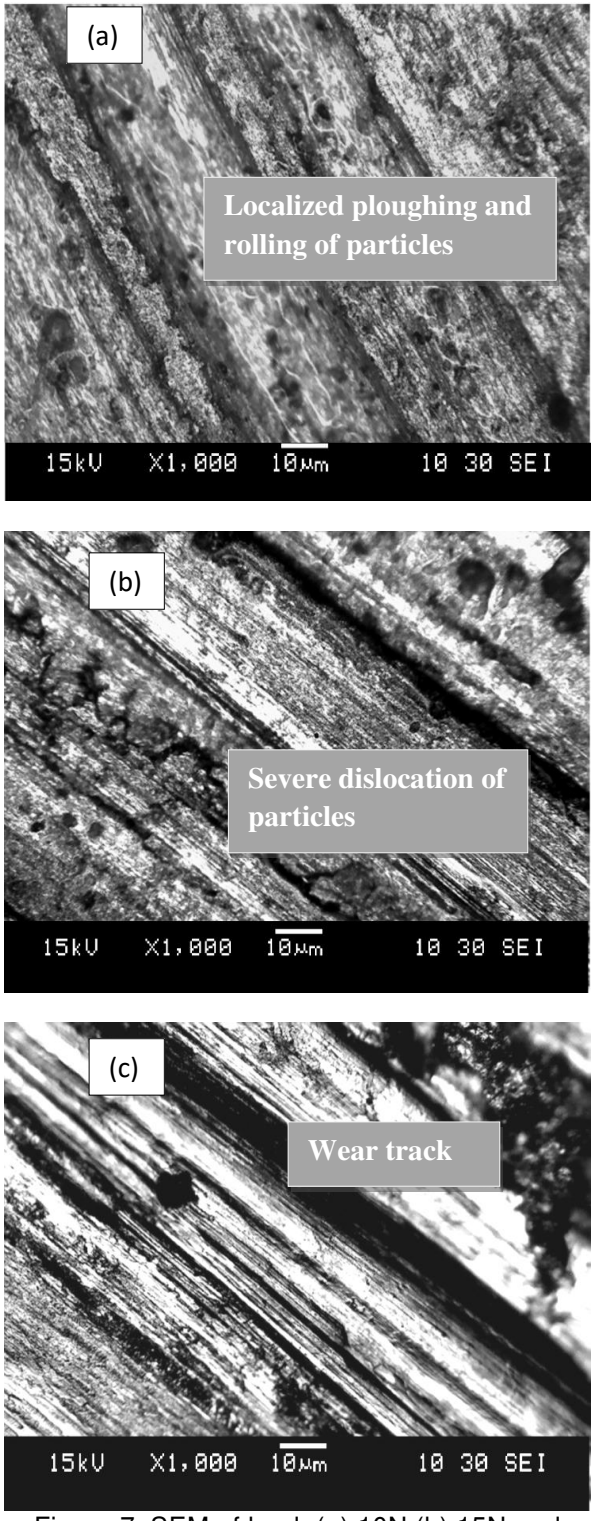

Figure 7. SEM of load: (a) 10N (b) 15N and (c) 20N shows dry wear and worn condition of the top layer under normal load

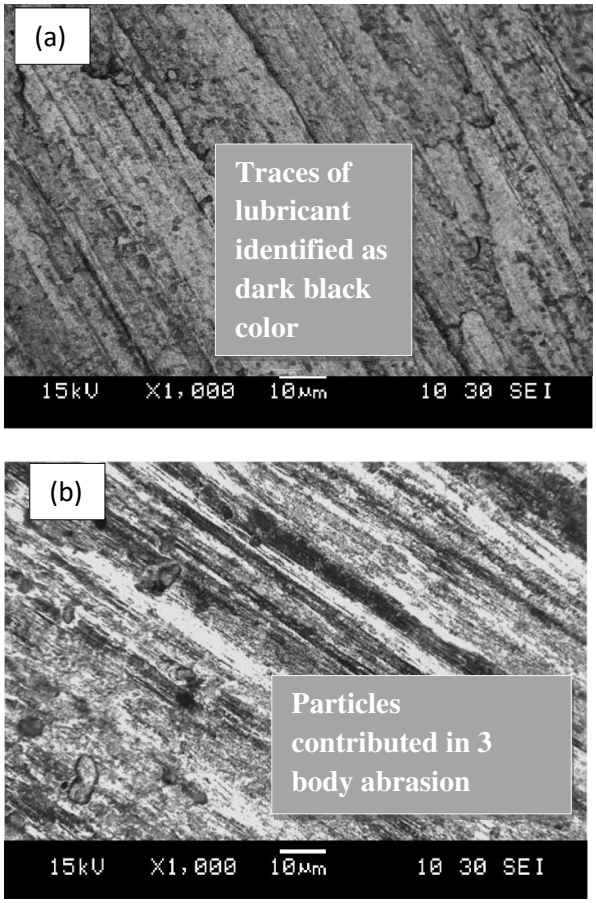

Figure 8. SEM of wet- post wear status of the topcoat at: (a) 10N (b) 15N and (c) 20N normal load

The motive of the make bigger in the slope is directly associated with the increase in wear rate. At the same time, the decomposing particles might also be due to the continuous formation, which stays in the layer of the mixture. While reading friction and wear, it was once found that at a regular 10N load, a better average could be predicted with and lubrication. The cause of several resistances to wear at the start a layer between the corroded surface of disc and pin and that continuation of the process leading to the surface hardness which leads to decrease wear.

Table 4. Average wear rate calculation under dry condition

Load in (N)	Avg. wear rate with lubricant $mm^3/m\times10^{-6}$	Avg. wear rate without lubricant $mm^3/m\times10^{-6}$
10	0.022	0.048
15	0.102	0.052
20	0.254	0.230

Table 5. Average wear rate calculation under wet condition

Load in (N)	Wear rate test 1 ($mm^3/m\times10^{-6}$)	Wear rate test 2 ($mm^3/m\times10^{-6}$)	Wear rate test 3 ($mm^3/m\times10^{-6}$)	Avg. wear rate with lubricant ($mm^3/m\times10^{-6}$)
10	0.0177	0.0272	0.033	0.024
15	0.1003	0.077	0.146	0.104
20	0.231	0.272	0.305	0.261

Table 6. Average wears rate calculation with and without lubricant at normal load of 10, 15 & 20 N

Load in (N)	Wear rate test 1 ($mm^3/m\times10^{-6}$)	Wear rate test 2 ($mm^3/m\times10^{-6}$)	Wear rate test 3 ($mm^3/m\times10^{-6}$)	Avg. wear rate without lubricant ($mm^3/m\times10^{-6}$)
10	0.052	0.054	0.031	0.043
15	0.036	0.031	0.081	0.051
20	0.291	0.264	0.135	0.232

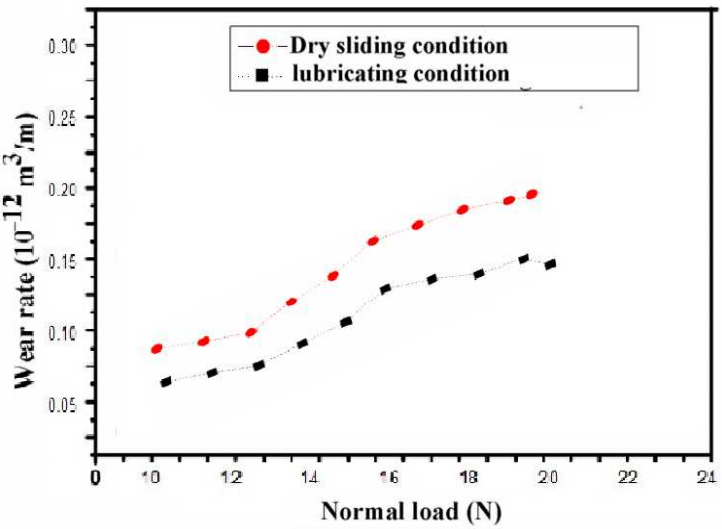

Figure 9. Comparative analysis of average wear rate with and without lubricant at the normal load of 10, 15, & 20 N

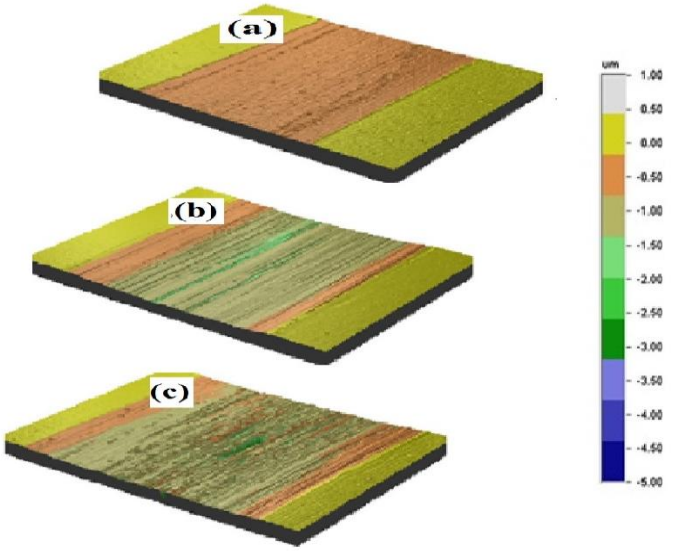

Figure 10. AFM showing micro indentation at the top coating of the wear tracks after test (a) Ra= 1.18 ± 0.05 µm (b) Ra= 7± 0.05 µm (c) Ra= 8.20 ± 0.05 µm, at 20 N

Figure 9 comparative analysis of the average wear rate with and without lubrication at normal loads of 10, 15 and 20 N. With lubricating oil, it can be regarded as a vital factor in changing wear rate under 15N load and under the lubricating oil, it gradually decreased to 0.051. X 10^{-6} mm ^{3}/m.

Figure 10, AFM shows a microprotrusion at the top coating under load (10, 15 and 20) N. The effect of extreme concentrations of these two elements could not be investigated. The similarity of some coatings also allowed us to see if there were internal differences in performance between similar coatings, which may explain to some extent the mixed results reported in the literature. This coating is associated with the roughness and, as a result, higher with additional surface roughness resulting in large bubbles. It is a large porosity substrate, superporous coatings are obtained. Comparing coatings made on a traditional sample, you can see that coatings applied to low porosity specimens are smoother. This truth can be determined by the microstructure of the substrate [29][30].

CONCLUSION

The conclusions related to verifying the dry and wet abrasive residences of the contemporary surface layer $Al2O_3$ ZrO_2 are as follows. First, this coating is of ordinary wear behavior from 10 to 15N, and it is virtually determined at high loads. From SEM microscope and under lubricating, the

wear rate was much less than 0.051 x 10^{-6} mm^3 / m. Then, lubricating oil can be regarded as a vital factor in changing wear rate under 15N load. In the dry state, the wear used to be 0.107 x 10^{-6} mm^3 / m, and under the lubricating oil, it gradually decreased to 0.051. X 10^{-6} mm ^{3}/m. Lubrication at 20N was used to decrease the wear rate. (Heavy signs and symptoms of wear). Finally, the wear decreases from 0.1732 X 10^{-6} mm ^{3}/m to 0.0665 X 10^{-6} mm ^{3}/m by roughness low.

ACKNOWLEDGMENT

This work used to be supported by way of the college of engineering, the University of Samarra. The authors would like to thank the University of Malaysian Science (USM) for the place all the exams had been finished in their laboratories.

REFERENCES

[1] J. Zhang and H. Li, "Influence of manganese phosphating on wear resistance of steel piston material under boundary lubrication condition," *Surface and Coatings Technology,* vol. 304, pp. 530–536, 2016, doi: 10.1016/j.surfcoat.2016.07.065

[2] D. Ernens, M.B. de Rooji, H.R. Pasaribu, E.J. van Riet, W.M. van Haaften, and D. J. Shipper, "Mechanical characterization and single asperity scratch behaviour of dry zinc and manganese phosphate coating," *Tribology International,* vol. 118, pp. 474-483, 2018

[3] A Fernie et al., "Joining of engineering ceramics," *International Materials Reviews*, vol. 5, no. 5, pp. 283-281, 2013, doi: 10.1179/174328009X461078

[4] T. Fett and D. Munz, "Ceramics: Mechanical Properties, Failure Behaviour, Materials Selection," *Springer,* ISBN: 978-3-642-63580-9, Corrected 2nd printing, 2011.

[5] Abhinav et al., "Corrosion kinetics of Al2O3+ZrO2·5CaO coatings applied on gray cast iron Substrate," *Ceramic International*, vol. 43, no. 17, pp.15708-15713, 2017, doi: 10.1016/j.ceramint.2017.08.131

[6] M. R. Loghman- Estarki et al., "Plasma-sprayed nanostructured Scandia-yttria and ceria-yttria codoped zirconia coatings: Microstructure, bonding strength and thermal insulation properties," *Ceramic International,* vol. 44, no. 11, pp. 12042-12047, 2017, doi: 10.1016/j.ceramint. 2018.03.204

[7] P. J. Blau, "Friction and wear transitions of materials," *Noyes publications,* Park Ridge, NJ, Year 1989.

[8] N. Krishnamurthy, et al., "Characterization and wear behavior of plasma-sprayed Al2O3 and ZrO25CaO coatings on cast iron substrate," *Journal of Material Science,* vol. 45, pp. 850–858, 2010

[9] M. S. Murali, Krishnamurthy et al., "A Study of Parameters Affecting Wear Resistance of Alumina and Yttria Stabilized Zirconia Composite Coatings on Al-6061 Substrate," *International Scholarly Research Network ISRN Ceramics*, pp.1-13, 2012, doi: 10.5402/2012/585892

[10] G. J. Gore and J. D. Gates, "Effect of hardness on three very different forms of wear," *Wear,* vol. 203-204, pp. 544-563, doi: 10.1016/S0043-1648(96)07414-5.

[11] I. Sevim, et al., "Effect of fracture toughness on abrasive wear resistance of steels," *Materials & Design*, vol. 27, no. 10, pp. 911-919, 2006, doi: 10.1016/j.matdes.2005. 03.009.

[12] L. Zhou, G. Liu, Z. Han and K. Lu, "Grain size effect on wear resistance of a nanostructured AISI 52100 steel," *Scripta Materialia*, vol. 58, no. 6, pp. 445-448, 2008, doi: 10.1016/ j.scriptamat.2007.10.034

[13] A. V. Makarova, N. N. Soboleva et al., "Role of the strengthening phases in abrasive wear resistance of laser-clad NiCrBSi coatings," *Journal of friction and wear*, vol. 38, pp. 272–278, 2017, 0.3103/ S1068366617040080.

[14] H. Liu and M. E. Fine, "Modelling of grain size dependent microstructure controlled sliding wear in polycrystalline alumina," *Journal of American Ceramic Society,* vol. 76, pp. 2392-2396, 1993.

[15] S. J. Cho, B. J. Hockey, B. R. Lawn, and S. J. Bennison, "Grain size and R-curve effects in the abrasive wear of alumina," *Journal of American Ceramic Society,* vol.72, pp.1249-1252, 1989, doi: 10.1111/j.1151-2916. 1989.tb09718.x

[16] R. A Al-Samarai, K. R. Ahmad, Haftirman, and Y. Al-Douri, ''The influence of roughness on the wear and friction coefficient under dry and lubricated sliding." *International Journal of Scientific and Engineering Research,* vol. 3, no. 4, pp. 1-6, 2012

[17] Y. Al-Douri, R. A. Al-Samarai, S. A. Abdulateef, A. A. Odeh, N. Badi, and C. H. Voon, "Nanosecond pulsed laser ablation to synthesize GaO colloidal nanoparticles," *Optik - International Journal for Light and Electron,* vol. 178, pp. 337-342, 2019, doi: 10.1016/j.ijleo.2018.09.158

[18] R. A. Al-Samarai and Y. Al-Douri, "Lubricated Conditions Imposed on Coating

Multi-layer on Wear Resistance under Cr2O3 Effect," *Materials Research,* vol. 21, no. 4, 2018, doi: 10.1590/1980-5373-mr-2017-0938

[19] H. K. Xu and S. Jahanmir, "Microfracture and material removal in scratching of alumina," *Journal of Materials Science*, vol. 30, pp. 2235-2247, 1995, doi: 0.1007/BF01184566

[20] L. Fan et al., "Wear Behavior of ZTA Reinforced Iron Matrix Composites," *Proceedings of the 7th International Conference on Fracture Fatigue and Wear, Fracture, Fatigue and Wear* FFW, Singapore, 2018, pp.732-74, doi: 10.1007/ 978-981-13-0411-8_65

[21] N. Singh et al., "Wear Behavior of ZrO2 Particle Reinforced (Fe,Ni) Matrix Composite," *Proceedings of the 7th International Conference on Fracture Fatigue and Wear, Fracture, Fatigue and Wear* FFW 2018, Singapore, 2018, pp. 682-690, doi: 10.1007/978-981-13-0411-8_61

[22] Abhinav et al., "An elucidation on adhesive strength of Al2O3 and ZrO2·5CaO composite coating applied on Al-6061 & CI substrates," *International Journal of Mechanical and Production Engineering Research and Development*, Special Issue, pp.91-98, June 2018, doi: 10.13140/ RG.2.2.17125.45281

[23] Abhinav et al., "Thermochemical and Thermomechanical Study on Composite Coatings (Al2O3+ZrO2·5CaO)," *International Journal of Recent Technology and Engineering,* vol. 8, no. 1C, May 2019.

[24] ASTM G132 standard, 100 Barr Harbor Drive, *West Conshohocken*, PA 19428-2959, United States.

[25] H. Liu and M. E. Fine, "Modelling of grain size dependent microstructure controlled sliding wear in polycrystalline alumina," Journal of American Ceramic Society, vol. 76, pp. 2392-2396, 1993.

[26] S. M. Weiderhorn and B. J. Hockey, "Effect of material parameters on the erosion resistance of brittle materials," *Journal of Materials Science,* vol.18, pp. 766-789, 1983, doi: 10.1007/BF00745575

[27] S. Lathabai and D. D. Pender, "Microstructural influence in slurry erosion of ceramics," *Wear*, vol.189, pp. 122-135, 1995.

[28] S. J. Cho, B. J. Hockey, B. R. Lawn et al., "Grain size and R-curve effects in the abrasive wear of alumina," *ournal of the American Ceramic Society*, vol. 72, no. 7, pp. 1249-1252, 1989, doi: 10.1111/j.1151-2916.1989.tb09718.x

[29] W. Chen, Q. Di, H. Zhang, F. Chen, and W. Wang, "The sealing mechanism of tubing and casing premium threaded connections under complex loads," *Journal of Petroleum Science and Engineering,* vol. 171, pp. 724-730, 2018, doi: 10.1016/j.petrol.2018.07.079

[30] A. Nevosad, S. Azhaarudeen, N. Doerr, H. Zacharias, J. Klarner, and E. Badisch, "Initial damage mechanism and running-in behaviour of phosphate conversion coatings," *Key Engineering Materials,* vol. 721, pp. 356–361, 2017, doi: 10.4028/ www.scientific.net/KEM.721.356